frontiers in Mechanical Engineering

ORIGINAL RESEARCH
published: 24 May 2021
doi: 10.3389/fmech.2021.681120

Multi-Technique Investigation of a Biomimetic Insect Tarsal Adhesive Fluid

J. Elliott Fowler[1], *Stanislav Gorb*[2] *and Joe E. Baio*[1]*

[1] The School of Chemical, Biological and Environmental Engineering Department, Oregon State University, Corvallis, OR, United States, [2] Department of Functional Morphology and Biomechanics, Zoological Institute of the University of Kiel, Kiel, Germany

There is substantial motivation to develop novel adhesives which take advantage of the superior adhesive strength and adaptability of many natural animal adhesives; however, the tools typically used to study these mechanisms are incapable of determining the precise interactions of molecules at an adhesive interface. In this study, a surface specific, order sensitive vibrational spectroscopy called sum frequency generation (SFG) is, for the first time, combined with multiple bulk characterization techniques to examine a novel, simple biomimetic adhesive fluid inspired by tarsal fluid of insects. Insects perform complex adhesive demands, including sticking, climbing vertically and running upside-down with little difficulty. Thus, we hypothesize that both bulk and surface specific properties of the fluid contribute to the success of this wet adhesive mechanism. SFG spectra of biomimetic emulsion exhibited similar hydrocarbon organization on hydrophobic and hydrophilic substrates to natural beetle fluid previously studied with the same method. Bulk characterization techniques indicated that the emulsion had a shear-thinning profile with the ability to enhance traction forces during climbing and low surface tension ideal for surface wetting on the majority of natural surfaces. Multi-technique comparisons between emulsion and pure squalane revealed that a hydrocarbon only based fluid could not replicate the traction promoting properties of the emulsion. We conclude that the insect tarsal fluid adhesive mechanism relies upon contributions from both surface-specific properties optimizing traction force and bulk properties promoting rapid surface wetting and maintaining pull-off force for fast detachment.

Keywords: bioadhesion, biomimetic, surface analysis, vibrational spectroscopy, insect adhesion

OPEN ACCESS

Edited by:
Yu Tian,
Tsinghua University, China

Reviewed by:
Ivan Argatov,
Technical University of Berlin, Germany
Feodor M. Borodich,
Cardiff University, United Kingdom

***Correspondence:**
Joe E. Baio
joe.baio@oregonstate.edu

Specialty section:
This article was submitted to Tribology, a section of the journal Frontiers in Mechanical Engineering

Received: *15 March 2021*
Accepted: *27 April 2021*
Published: *24 May 2021*

Citation:
Fowler JE, Gorb S and Baio JE (2021) Multi-Technique Investigation of a Biomimetic Insect Tarsal Adhesive Fluid. Front. Mech. Eng. 7:681120. doi: 10.3389/fmech.2021.681120

INTRODUCTION

Within biological evolution, numerous adhesive systems developed for millions of years. The inspiration from studies of one type of such systems, insect tarsal adhesion, has led to improvements in materials design, such as reversibly-adhering sticky tapes and climbing robots (Gorb et al., 2007; Daltorio et al., 2009). These improvements have been mainly focused on mimicry of the details of the physical structure of insect feet. However, this system additionally contains a fluid secreted from insect pads which mediates contact between foot and surface (Walker, 1993; Dirks and Federle, 2011). Many previous studies have shown that this fluid is vital to the ability of insects to walk and

climb without slipping and sliding on various natural and artificial surfaces (Gorb, 2001; Gorb and Gorb, 2002, 2009; Langer et al., 2004; Gorb et al., 2008, 2010; Busshardt et al., 2012; Hosoda and Gorb, 2012; England et al., 2016). However, a consensus explanation for precisely how this fluid aids both strong adhesion and rapid release does not currently exist (Gilet et al., 2018).

The composition of the tarsal fluid in various insect species has been analyzed directly, using techniques, such as mass spectrometry, and indirectly by assessing its interaction with various chemicals and surfaces (Geiselhardt et al., 2009, 2010, 2011; Gorb et al., 2010; Peisker and Gorb, 2012; Heepe et al., 2016). Mass spectrometry results have concluded that insect adhesive fluid consists of a mixture of branched and unbranched, long and short chain hydrocarbons, fatty acids, sugars, and alcohols (Vötsch et al., 2002; Geiselhardt et al., 2011). Microscopy data suggests insect adhesive fluids to be oil-in-water emulsions. Indeed, this would be an ideal contacting fluid for its ability to spread easily on a wide range of substrates (Peisker et al., 2014). Manipulations of the tarsal fluid of the Colorado Potato Beetle (*Leptinotarsa decemlineata)*, as well as traction force experiments of Seven-Spotted Ladybird Beetles (*Coccinella septempunctata*) on nanoporous substrates, showed that removal of just part of the fluid significantly diminished their adhesive forces (Geiselhardt et al., 2010; Gorb et al., 2010). Additionally, studies have consistently demonstrated that there was a complex relationship between the chemistry of insect adhesive fluid and the chemistry of the contacting surface (Federle et al., 2002; Dirks and Federle, 2011; England et al., 2016).

Recently, natural *C. septempunctata* fluid was studied with sum frequency generation (SFG) spectroscopy—a surface specific, order sensitive vibrational spectroscopy—on surfaces with a range of wettabilities, to determine what molecular groups were surface active and ordered at the interface. It was hypothesized that interfacial chemistry and molecular order were dynamic; however, it was instead found that interfacial fluid consisted of ordered hydrocarbons regardless of substrate hydrophilicity. It was concluded that the hydrocarbons were a mixture of branched and unbranched alkanes which were more highly ordered at hydrophobic interfaces, decreasing traction force of the beetles, thus enhancing lubrication. Nevertheless, this study did not reveal a clear mechanism that solely explained the functional mechanism of the beetle tarsal fluid adhesion.

Therefore, in this study we designed a biomimetic insect adhesive fluid with the distinct aim of deducing the mechanism that enabled natural insect tarsal fluid to generate necessary adhesive forces. We hypothesized that the fluid must take advantage of both surface and bulk properties to maximize traction force while generating appropriate pull-off force. Thus, we believed that both the surface active and surface-inactive components of the emulsion played an important role in the insect tarsal adhesive mechanism.

A simple, three-component biomimetic adhesive emulsion was formulated from squalane, deuterated stearic acid and D_2O, chosen such that each component contained distinct chemical bonds which could be probed at the fluid-substrate interface. This emulsion was initially characterized with dynamic light scattering, surface tensiometry and rheology. SFG spectroscopy was then used to probe C-H, O-D, C-D and C=O vibrations at the interface between the biomimetic fluid and two surfaces—hydrophobic polystyrene and hydrophilic polyethylene oxide—to determine the effect of substrate chemistry on organization of surface active fluid molecules. The fluid was then iteratively deconstructed to determine the influence of the surface-inactive components on the organization of the surface-active layers of the fluid.

MATERIALS AND METHODS

Emulsion Formulation

Ten mL of squalane (96% purity, Sigma Aldrich, St. Louis, MO) was added to a scintillation vial cleaned by rinsing with ethanol and heated to 70°C. A 1 mM deuterated stearic acid in squalane solution was made by adding 3.2 mg of stearic-d_{35} acid (98 atom% d, Sigma Aldrich) and mixing with a magnetic stir-bar at 1,000 rpm. Finally, 0.5 mL of D_2O was added dropwise and allowed to mix for 3 min. Emulsions were formed by ultrasonication at 60°C for 2 min. All experiments were performed with freshly made emulsion.

Rheological and Tribological Characterization of Fluids

The rheological behavior of the formulated emulsion, as well as pure squalane, was determined using a DHR3 Rheometer (TA Instruments, New Castle, DE) in cone-and-plate geometry with a 60 mm, 1.01°, titanium Peltier plate. Flow sweeps were performed at 25°C by measuring the viscosity and shear stress of the fluids while varying the shear rate from 1×10^{-3} to 1,000 s^{-1}. Pull-off force measurements were performed in plate-plate geometry with a 20 mm, titanium plate and an initial gap size of 300 μm. The gap was filled with either emulsion or squalane and the axial force was zeroed. The top plate was lifted at a rate of 300 μm/s and the minimum axial force measured was reported as the pull-off force.

Surface Tensiometry

The surface tension of the emulsion and precursor fluids was measured with an FTA-T10 tensiometer (First Ten Angstroms, Portsmouth, VA) using a Du Nouy Ring. The reported surface tension was the average of ten consecutive dipping cycles. Measurements began only after a consistent force per wetted length peak was achieved.

Substrate Preparation

Fifteen millimeter diameter CaF_2 optics (International Crystal Laboratories, Garfield, NJ) were cleaned via successive ultrasonication in dichloromethane, acetone and ethanol and spun-coat (Laurell Technologies, North Wales, PA) at 2,000 rpm for 60 s with 3 wt% solutions of one of the following: polyethylene oxide (PEO, MW = 100,000 Da) (Sigma Aldrich), polystyrene (PS, MW = 35,000 Da) (Sigma Aldrich), deuterated poly-ethylene oxide (dPEO, MW = 8,960 Da) (Polymer Source Inc., Montreal, CA) or deuterated polystyrene (dPS, MW = 7,420 Da) (Polymer Source Inc.) in toluene. Films were

then baked at 80°C for 20 h at 500 mtorr to remove excess solvent. We have previously shown that this produced optically transparent polymer films of ∼100 nm in thickness. Substrates were stored under N_2 atmosphere in sealed Petri dishes until use to prevent contamination.

Sum Frequency Generation Spectroscopy

An EKSPLA Nd:YAG laser, operating at 50 Hz, was used to generate both a fixed visible (532 nm^{-1}) and tunable IR beam (1,000–4,000 cm^{-1}) via sequential pumping through an EKSPLA optical parametric generation/amplification and difference frequency unit, which utilized barium borate and AgGaS2 crystals, respectively. The visible and IR beams (∼150 μJ/pulse) were overlapped spatially and temporally at the desired interface to generate SFG photons, which were spectrally filtered, dispersed by a monochromator and detected with a gated photomultiplier tube. Both beams were focused to a ∼1 mm diameter at the interface. Spectra were collected in 4 cm^{-1} steps with 400 acquisitions per step.

SFG spectra were generated at two different polarization combinations – ssp (s-polarized SFG, s-polarized visible, p-polarized IR) and ppp (p-polarized SFG, p-polarized visible, p-polarized IR) in four different vibrational regions (C-H – 2,800–3,100 cm^{-1}; D-O – 2,450–2,650 cm^{-1}; C=O – 1,600–1,800 cm^{-1}; C-D – 2,000–2,300 cm^{-1}) through the backside of a CaF2 window which rests on a Teflon o-ring (ID – 7.9 mm) attached to a flat, cylindrical Teflon platform. The void volume of the o-ring was filled with the sample fluid such that the fluid was in full contact with the top window surface at all times during the experiment. SFG signal is optimized in each wavenumber region using an Au-coated CaF_2 window in the same set-up. The fitting routine for SFG spectra is previously detailed elsewhere (Weidner et al., 2010; Baio et al., 2012, 2015; Weidner and Castner, 2013). Briefly, spectra were iteratively fit to the equation below (Equation 1) to determine non-resonant phase, non-resonant background (χ_{nr}), frequency (ω_q), individual peak full width half maximum (FWHM; Γ_q) and individual peak amplitude (A_q).

$$\chi^{(2)}_{eff} = \chi_{nr} + \sum_{q} \frac{A_q}{\omega_2 - \omega_q + i\Gamma_q} \quad (1)$$

RESULTS

Emulsion Characterization

From visual observation, the emulsion was stable over short periods of time (hours) but was susceptible to aggregation of the particle phase overnight. Particle aggregation was supported by dynamic light scattering measurements, which determined the mean particle size of the emulsion to be 8.0 μm with a polydispersity index of 0.4. This indicated a suspension on the borderline between a medium and broad distribution of particle sizes (Aragon and Pecora, 1976). Additionally, particles of various sizes were clearly visible in light microscope images of fresh emulsion (**Figure 1**).

Next, the surface tensions of emulsion as well as two control fluids, pure squalane and a 1 mM d-stearic acid in squalane solution, were determined (**Supplementary Table 1**). The surface tension of pure squalane was measured at 28.4 ± 0.1 mN/m, which was consistent with the reported literature value of 28 mN/m (Korosi and Kovats, 1981). The surface tension of the 1 mM d-stearic acid in squalane solution was lower at 27.1 ± 0.1 mM/m, which was expected due to the amphiphilic nature of stearic acid (Cho et al., 2018). Finally, the emulsion had a surface tension of 27.5 ± 0.1 mN/m. Overall, the surface tensions of all three fluids were consistent with the estimated surface tension of a hydrophobic secretion (∼30 mN/m) (Federle et al., 2004).

Rheometry experiments of both the emulsion and pure squalane revealed distinctly different viscosity profiles. Unsurprisingly, the viscosity of a film of pure squalane was constant (29 mPa*s) across a wide range of shear rates, which was consistent with the many previous analyses of the hydrocarbon as a low viscosity Newtonian fluid (Gupta et al., 1998). However, viscosity measurements taken from a film of emulsion provided a shear-thinning profile, with a very small yield stress of ∼0.01 Pa. Additionally, a plate-plate geometry was used to determine the pull-off adhesive strength of the two fluids. There was no difference in the tackiness of the emulsion compared to the hydrocarbon, with forces of 0.533 ± 0.009 and 0.527 ± 0.007, respectively (**Supplementary Table 2**).

SFG Spectroscopy

As previously mentioned, the composition of the emulsion was carefully selected to allow for isolation of representative molecular bonds from each component in separate vibrational regions, which were measured with SFG spectroscopy. This allowed for the determination of which components in the fluid were surface active. For example, the C-H stretching region (2,800–3,000 cm^{-1}) was used to measure ordered modes at the interface corresponding to squalane as the only source of methyl and methylene modes was that component of the emulsion. Likewise, the O-D stretching region (2,450–2,650 cm^{-1}) was used to observe D_2O at the interface, while the C-D (2,000–2,350 cm^{-1}) and C=O (1,650–1,800 cm^{-1}) regions were for observing d-stearic acid vibrational modes.

SFG spectra of emulsion at dPEO and dPS surfaces in SSP polarization combination at the C-H stretching region are shown in **Figure 2B**. Four vibrational modes were observed in both spectra: near 2,855, 2,880, 2,914, and 2,935 cm^{-1}, corresponding to CH_2 symmetric, CH_3 symmetric, CH_2 asymmetric, and CH_3 Fermi modes, respectively (Himmelhaus et al., 2000; Chen et al., 2003; Ma and Allen, 2006; Baio et al., 2015; Adams et al., 2017). All of these modes were also observed in SSP, C-H region spectra of the natural *C. septempunctata* fluid on the same substrates, except for the CH_2 asymmetric mode (**Figure 2A**). Spectra of the emulsion at the same surfaces in PPP polarization combination produced substantially different spectral profiles. Five total modes were observed in PPP spectra: near 2,864, 2,884, 2,900, 2,925, and 2,962 cm^{-1} corresponding to CH_2 symmetric, CH_3 symmetric, CH (tertiary), CH_2 asymmetric, and CH_3 asymmetric vibrational modes, respectively (**Supplementary Figure 1**). However, unlike in SSP combination, the same set of modes was not present across spectra of fluid on both surfaces, with the CH_2 and CH_3

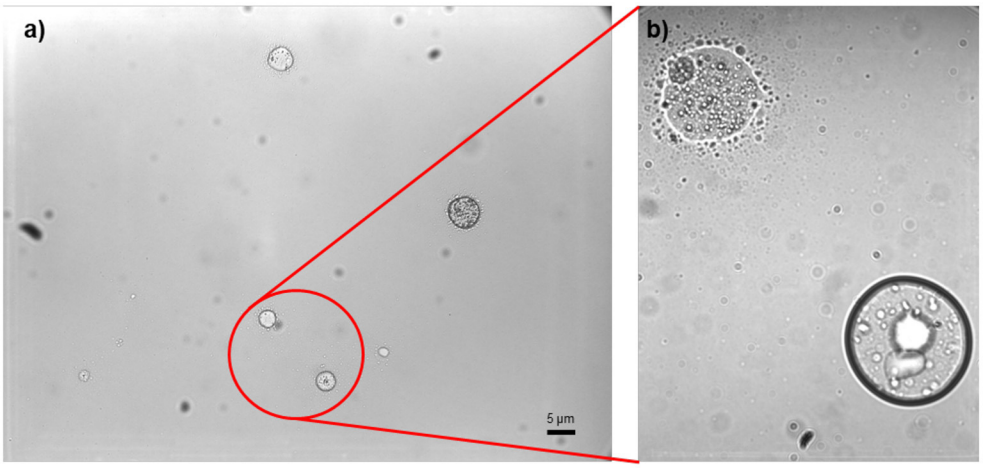

FIGURE 1 | Phase contrast light microscope image of the biomimetic emulsion at 10× **(a)** and 50× **(b)** magnifications. Insect feet fluids are usually emulsions at the nanoscale: one cannot see the second phase in optical microscope, only in an electron microscope (SEM, TEM) or in an atomic force microscope (AFM).

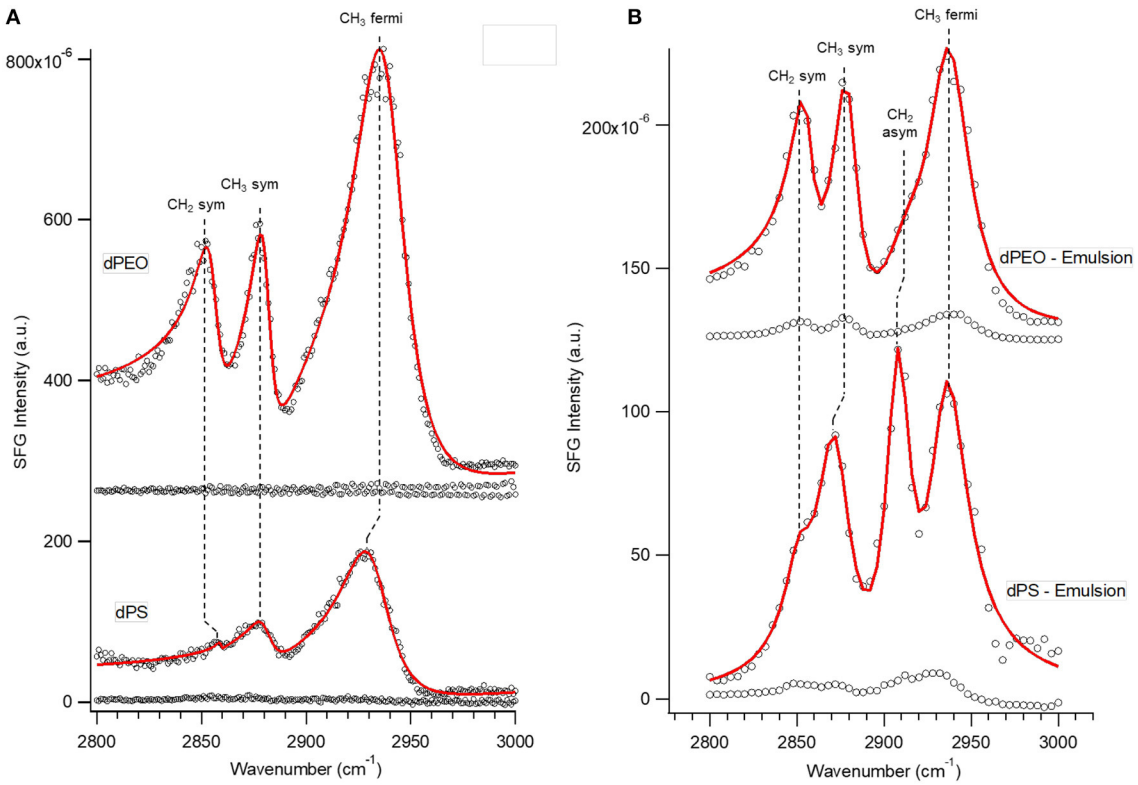

FIGURE 2 | SFG spectra in the C-H stretching region and SSP polarization combination of **(A)** natural beetle *Coccinella septempunctata* tarsal fluid on PEO and PS substrates and **(B)** biomimetic emulsion on PEO and PS substrates. Three vibrational modes were observed in all four spectra: near 2,855, 2,880, and 2,935 cm^{-1} corresponding to CH_2 symmetric, CH_3 symmetric, and CH_3 Fermi vibrational modes, respectively. One mode is unique to the biomimetic emulsion/substrate interfaces, the CH_2 asymmetric stretch near 2,914 cm^{-1}, likely due to different orientation of surface hydrocarbons between natural and biomimetic fluids. Relative SFG intensity of CH_3 and CH_2 symmetric modes and the change in this intensity as hydrophobicity is increased is similar between natural and biomimetic fluid interfaces.

symmetric and CH_2 asymmetric modes absent in the emulsion – dPS spectrum.

The relative ratio of CH_3 symmetric to CH_2 symmetric stretch amplitudes has been shown to be indicative of the relative organization of a layer of hydrocarbons, with larger values indicating a more uniform angle in relation to the surface (Casford et al., 2014; Adams et al., 2017). These values, and the trend between substrates, were similar for the same substrates in the natural and biomimetic fluid spectra, with values of 3.46 ± 0.40 and 1.03 ± 0.07 for the dPS and dPEO spectra of the natural fluid and $4.47 \pm$ and $1.70 \pm$ for spectra of the same surfaces with biomimetic fluid. However, there was one major difference between the C-H SSP spectra of the natural and biomimetic fluids – the presence of a peak corresponding to CH_2 asymmetric stretching near 2,914 cm^{-1} in the latter (**Figure 2B**). Previous SFG studies of alkane chains oriented toward the surface normal at solid/air and liquid/air interfaces have shown that the CH_2 asymmetric stretch has a substantially lower intensity in SSP compared to PPP or SPS polarization combinations. In this study, this trend was reversed, with stronger peak amplitude in SSP than PPP spectra. The mode amplitude was particularly strong at the hydrophobic surface – at which squalane would interact with more favorably. One explanation for this result is that squalane has been shown, via molecular dynamics (MD) simulations for squalane on hydrophilic silicon, to prefer a chain orientation parallel to solid surfaces with its methyl side chains arranged perpendicular from the chain (**Figure 3**) (Mo et al., 2005; Tsige and Patnaik, 2008). As mode amplitudes are sensitive to beam polarization as well as molecular bond orientation and order, it follows that a substantial rotation in chain angle could have led to the observed shifting in preference for the CH_2 asymmetric stretch from PPP to SSP polarization combination (Hirose et al., 1993). Thus, although organization of squalane chains at the emulsion interface was consistent with organization of hydrocarbons in natural adhesive fluid, the squalane layers were rotated perpendicularly from the natural fluid hydrocarbons. Lastly, spectra of the emulsion at non-deuterated substrates collected in the other three (O-D, C-D, C=O) stretching regions did not produce any SFG signal originating from either the D_2O or d-stearic acid molecules at either substrate (**Supplementary Figures 2**, **3**). This was consistent with characterizations of natural *C. septempunctata* fluid, in which hydrocarbons were shown to be the only surface-active component.

Next, spectra of pure squalane and a 1 mM d-stearic acid in squalane solution at PEO and PS surfaces were compared to emulsion spectra to determine whether surface-inactive components of the emulsion (d-stearic acid, D_2O) influenced the organization of the interfacially-active squalane molecules. While spectra were collected in all four regions (C-H, O-D, C-D, C=O), we only observed signal in C-H region spectra for each of the control fluids. The four modes previously identified in C-H SSP spectra were present in both control fluids spectra; however, an additional mode was observed near 2,868 cm^{-1} (**Figure 4**). Due to the wave number proximity of this mode to the CH_3 symmetric mode near 2,880 cm^{-1}, we attributed this mode to the resonance created by the dimethyl branching at either end of squalane molecules. Interestingly, it was only clearly observed in pure squalane spectra for both surfaces (Bellany, 1975). There were distinctly different trends in amplitude for the CH_2 symmetric, CH_3 symmetric and CH_2 asymmetric modes observed between the hydrophobic and hydrophilic surfaces and across the set of fluids. For example, the CH_2 asymmetric stretch amplitude decreased from emulsion to squalane/d-stearic acid to squalane only spectra at the PS surface (**Figure 3B**); however, at the PEO surface, the amplitude was initially negligible, increased for the squalane/d-stearic acid solution and was then negligible again for squalane (**Figure 3A**). Similarly, on the PS surface the CH_2 symmetric stretch was greater for the control fluids compared to the emulsion, but on the PEO surface the amplitude initially decreased for the squalane/d-stearic acid solution and then increased substantially for squalane only. Overall, the mode amplitude trends in this experiment showed that the removal of an amphiphilic molecule and D_2O led to apparent changes in the organization of interfacial squalane, although the specific changes were unique to the wettability of the contacting surface. However, on both surfaces the emulsion spectra exhibited greater organization of interfacial squalane layers than pure squalane.

DISCUSSION

To evaluate the role of secreted tarsal fluid in the adhesion of insects, several factors must be taken into account. For instance, an insect standing upright and still on a flat vertical substrate must generate sufficient contact with the surface, to prevent sliding down, but must not generate sufficiently strong adhesive force that can hamper its detachment from the surface to proceed with the locomotion. This compromise is solved by the specific geometry of the setae (Niederegger and Gorb, 2003; Gorb, 2011), but the corresponding contribution from the molecular organization of the fluid can be additionally expected. An optimal adhesive fluid must be able to handle transitioning from wet to dry, smooth to rough, hydrophobic to hydrophilic or upright to inclined or inverted without failure. Thus, an ideal insect tarsal adhesive fluid would utilize a mechanism which was inherently complex – no single characteristic of the fluid responsible for mitigating all of the aforementioned challenges singularly.

While there have been many attempts to ascertain this mechanism using biomechanical experiments, surface analytical approaches have been underutilized. Thus, this study used SFG showing the organization of molecules within the biomimetic emulsion at the surface of hydrophobic and hydrophilic substrates. As previously introduced, this technique was also recently used to probe natural *C. septempunctata* tarsal adhesive fluid and it was found that a layer of branched and unbranched hydrocarbons organized at all substrate surfaces with organization dependent upon substrate wettability. It has been shown that beetles exhibited significantly different traction forces depending upon the wettability of the contacting surface (Gorb et al., 2008; Gorb and Gorb, 2009). An inverse relationship existed between the ordering of a layer of hydrocarbons at the interface and the magnitude of traction force measured on similar surfaces. Thus, it was concluded that the fluid enhanced traction force on

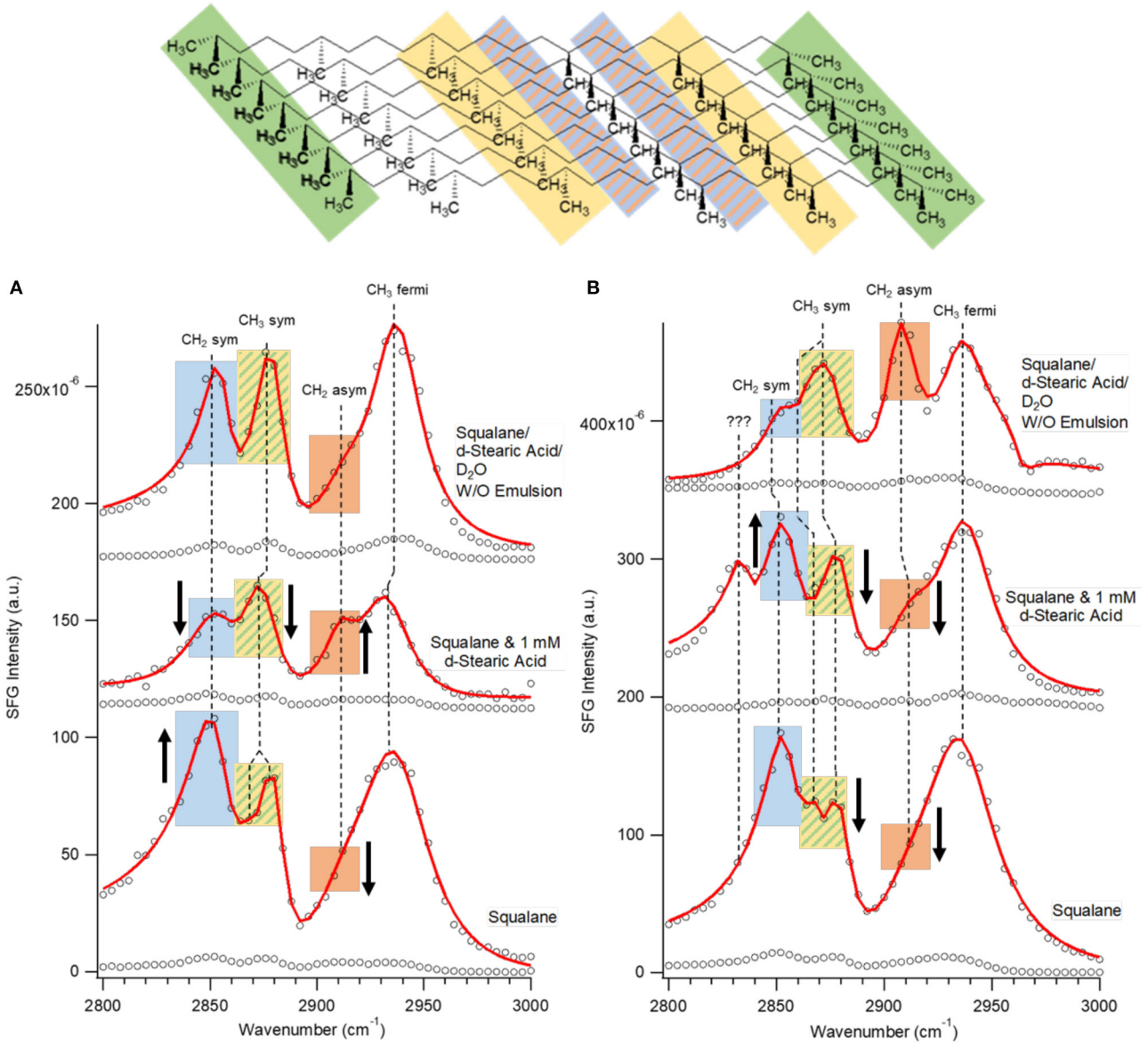

FIGURE 3 | SFG spectra of biomimetic emulsion and control fluids at PEO **(A)** and PS **(B)** surfaces in the C-H vibrational region and SSP polarization combination. Spectra and fits are represented by black circles and red dots, respectively. Five vibrational modes were observed in all of the spectra: near 2,855, 2,868, 2,880, 2,914, and 2,935 cm^{-1} corresponding to CH_2 symmetric, CH_3 symmetric, CH_2 asymmetric, and CH_3 Fermi vibrations, respectively. Colored bars indicate vibrational mode locations on a layer of squalane molecules present at the interface. Black arrows indicate relative change in mode amplitude from the same mode in the spectrum above it.

hydrophilic substrates, where an oily fluid would interact less strongly, and increased lubrication of hydrophobic substrates, where interactions would naturally be stronger.

Yet, limiting factors, such as the very small volume (pL) of fluid droplets and the certain volatility of some components of the fluid limited the ability to definitively conclude, whether chemical surface analytical results were representative of the complete mechanism (Peisker and Gorb, 2012). In this study, a biomimetic emulsion was created in quantities with which fluid volume and chemistry could be carefully controlled during SFG experiments. Resultant SFG spectra provided clear evidence that the hydrocarbon component, squalane, was the only substrate-active chemical in the emulsion. Additionally, the emulsion displayed very similar hydrocarbon chain organization (CH_3/CH_2 stretching ratios) to the natural *C. septempunctata* fluid (**Figure 2**). Both results supported the previous conclusion that a surface-active hydrocarbon component in beetle tarsal fluid was responsible for moderating traction and lubrication in response to changing environmental surface chemistry.

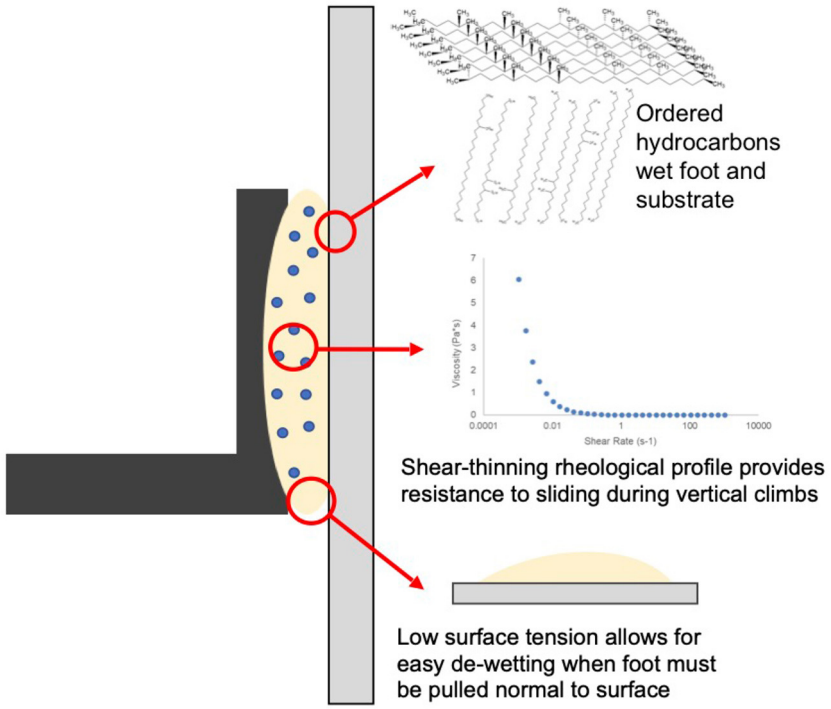

FIGURE 4 | The corresponding properties of natural and biomimetic insect tarsal adhesive fluid allowing fast attachment and detachment both essential for performing rapid locomotion.

However, rheological testing of the biomimetic fluid revealed an additional benefit of an emulsion in generation of traction force. The resistance of the vesicle phase against the bulk phase, when shear was applied, led to a shear-thinning non-Newtonian fluid with a small yield stress (**Supplementary Figure 4**) (Dirks et al., 2010). The higher viscosity exhibited by a fluid with this profile during events with very low or no shear rate, such as clinging on inclined surfaces or ceilings, would be ideal for slip prevention (Bullock et al., 2008; Dirks et al., 2010; Dirks and Federle, 2011). However, the shear rate applied by this system at average beetle walking speed (∼5 mm/s) and with a biomimetic fluid layer 100 nm thick (a conservative estimate of natural fluid thickness) (Gorb et al., 2012; Gilet et al., 2018) would be well above the rate necessary for the fluid to exhibit a constant, low viscosity like that of pure squalane (**Supplementary Figure 4**) (Thornham et al., 2008; Dirks and Federle, 2011). Thus, this fluid would provide a resistance to sliding without increasing the effort required to resume movement. Combined, a slip-resistant bulk structure and a lubricating surface layer sensitive to substrate chemistry indicated that the tarsal adhesive fluid mechanism is adapted to support the dynamic adhesion during locomotion (quick attachment and detachment).

It has been previously shown that some insect fluids may consist only of hydrocarbons (Gorb, 2001; Geiselhardt et al., 2010, 2011). Thus, it was necessary to determine whether a fluid consisting of only hydrocarbon molecules reasonably replicated the complete composition and adhesive properties of the biomimetic emulsion. Squalane, a low viscosity, low surface tension fluid has been shown to have low cohesive forces, which can be correlated to both easier filling of small asperities and faster de-wetting from a surface (Ludviksson and Lightfoot, 1971; Moore et al., 2000; Peisker et al., 2014). These properties would be desired for maximizing contact area and pull-off adhesive force. In fact, if the only consideration for adhesion was pull-off force and surface wetting, pure squalane may be considered an ideal mimic for beetle adhesive fluid. It generated the same pull-off force as the emulsion in this study while having a comparable surface tension (**Supplementary Figure 5** and **Supplementary Tables 1**, **2**).

However, we hypothesized that the shear force (often called traction or friction force in experimental studies on insects) is at least as important as these factors, if not more so (Labonte and Federle, 2015; Amador et al., 2017). Our comparison of the SFG spectra of emulsion vs. pure squalane on hydrophobic and hydrophilic substrates revealed clear differences in the organization of squalane layers between the two fluids on each substrate (**Figure 3**). Most importantly, the contrast in ordering ratio observed in both the emulsion and natural *C. septempunctata* fluid spectra were not present between the squalane spectra on each substrate. This should lead to the absence of the difference in traction force between the hydrophobic and hydrophilic substrates. However, this is inconsistent with biomechanical results obtained with living beetles. Thus, the emulsion was the only fluid which combined the low surface tension spreading advantages to control pull off force and the dynamic organizational response to substrate

hydrophobicity to optimize traction force. Furthermore, we have demonstrated that the surface inactive components of the biomimetic tarsal adhesive fluid—the water and stearic acid emulsion phase—clearly influence the organization of the surface active squalane layers and by extension the adhesive properties of the fluid.

CONCLUSIONS

Our previous experiments on natural beetle adhesive fluid (Fowler et al., 2021) and on the biomimetic fluid presented in this paper have shown that the interfacial interactions between the fluid and substrate are an important component of the foot adhesive mechanism, ensuring wetting during movement across the substrate surface as well as maintaining sufficient surface contact via low surface tension. However, chemistry of the bulk, surface-inactive fluid played an equally important role by bestowing a shear-thinning profile to the fluid and regulating the magnitude of traction forces generated by influencing order of the interfacial components.

An immediate application of biomimetic beetle tarsal adhesive is in the development of climbing robots, as the fluid resists shear well while generating relatively small pull-off forces. This would minimize the necessary energy input for successive climbs. However, additional work is still needed to improve the stability the oil-in-water emulsion. In this study, composition was limited to naturally occurring chemicals with very specific molecular bonds so that each chemical could be tracked. Future formulations may explore surfactants which have stronger affinities for water to prevent aggregation of vesicles above micron sizes. Regardless, herein we have shown that a combination of surface specific and bulk analytical techniques as well as work on artificial fluid systems inspired by biological ones can be used to understand details of a complex adhesive mechanisms developed by nature.

DATA AVAILABILITY STATEMENT

The raw data supporting the conclusions of this article will be made available by the authors, without undue reservation.

AUTHOR CONTRIBUTIONS

JEF, JEB, and SG: conceptualization. JEB and SG: supervision. JEF: investigation and writing—original draft preparation. JEF and JEB: methodology. JEB and SG: writing—review and editing.

FUNDING

This work was partially supported by German Science Foundation (DFG Grant GO 995/34-1 to SG) within Special Priority Program Soft Material Robotic Systems.

SUPPLEMENTARY MATERIAL

The Supplementary Material for this article can be found online at: https://www.frontiersin.org/articles/10.3389/fmech.2021.681120/full#supplementary-material

REFERENCES

Adams, E. M., Champagne, A. M., Williams, J. B., and Allen, H. C. (2017). Interfacial properties of avian stratum corneum monolayers investigated by Brewster angle microscopy and vibrational sum frequency generation. *Chem. Phys. Lipids* 208, 1–9. doi: 10.1016/j.chemphyslip.2017.08.002

Amador, G. J., Endlein, T., and Sitti, M. (2017). Soiled adhesive pads shear clean by slipping: a robust self-cleaning mechanism in climbing beetles. *J. R. Soc. Interface* 14:20170134. doi: 10.1098/rsif.2017.0134

Aragon, S., and Pecora, R. (1976). Theory of dynamic light scattering from polydisperse systems. *J. Chem. Phys.* 64, 2395–2404. doi: 10.1063/1.432528

Baio, J. E., Spinner, M., Jaye, C., Fischer, D. A., Gorb, S. N., and Weidner, T. (2015). Evidence of a molecular boundary lubricant at snakeskin surfaces. *J. R. Soc. Interface* 12, 1–8. doi: 10.1098/rsif.2015.0817

Baio, J. E., Weidner, T., Baugh, L., Gamble, L. J., Stayton, P. S., and Castner, D. G. (2012). Probing the orientation of electrostatically immobilized Protein G B1 by time-of-flight secondary ion spectrometry, sum frequency generation, and near-edge X-ray adsorption fine structure spectroscopy. *Langmuir* 28, 2107–2112. doi: 10.1021/la203907t

Bellany, L. (1975). The infrared spectra of complex molecules. London: *Chapman Hall,* 1p.

Bullock, J. M., Drechsler, P., and Federle, W. (2008). Comparison of smooth and hairy attachment pads in insects: friction, adhesion and mechanisms for direction-dependence. *J. Exp. Biol.* 211, 3333–3343. doi: 10.1242/jeb.020941

Busshardt, P., Wolf, H., and Gorb, S. N. (2012). Adhesive and frictional properties of tarsal attachment pads in two species of stick insects (Phasmatodea) with smooth and nubby euplantulae. *Zoology* 115, 135–141. doi: 10.1016/j.zool.2011.11.002

Casford, M. T. L., Ge, A., Kett, P. J. N., Ye, S., and Davies, P. B. (2014). The structure of lipid bilayers adsorbed on activated carboxy-terminated monolayers investigated by sum frequency generation spectroscopy. *J. Phys. Chem. B* 118, 3335–3345. doi: 10.1021/jp410401z

Chen, C., Loch, C. L., Wang, J., and Chen, Z. (2003). Different molecular structures at polymer/silane interfaces detected by SFG. *J. Phys. Chem. B* 107, 10440–10445. doi: 10.1021/jp035211f

Cho, H.-J. J., Sresht, V., and Wang, E. N. (2018). Predicting surface tensions of surfactant solutions from statistical mechanics. *Langmuir* 34, 2386–2395. doi: 10.1021/acs.langmuir.7b03749

Daltorio, K. A., Wei, T. E., Horchler, A. D., Southard, L., Wile, G. D., Quinn, R. D., et al. (2009). Mini-Whegs TM climbs steep surfaces using insect-inspired attachment mechanisms. *Int. J. Robot. Res.* 28, 285–302. doi: 10.1177/0278364908095334

Dirks, J.-H., Clemente, C. J., and Federle, W. (2010). Insect tricks: two-phasic foot pad secretion prevents slipping. *J. R. Soc. Interface* 7, 587–593. doi: 10.1098/rsif.2009.0308

Dirks, J.-H., and Federle, W. (2011). Fluid-based adhesion in insects - principles and challenges. *Soft Matter* 7, 11047–11053. doi: 10.1039/c1sm06269g

England, M. W., Sato, T., Yagihashi, M., Hozumi, A., Gorb, S. N., and Gorb, E. V. (2016). Surface roughness rather than surface chemistry essentially affects insect adhesion. *Beilstein J. Nanotechnol.* 7, 1471–1479. doi: 10.3762/bjnano.7.139

Federle, W., Baumgartner, W., and Hölldobler, B. (2004). Biomechanics of ant adhesive pads: frictional forces are rate- and temperature-dependent. *J. Exp. Biol.* 207, 67–74. doi: 10.1242/jeb.00716

Federle, W., Riehle, M., Curtis, A. S. G., and Full, R. J. (2002). An integrative study of insect adhesion: mechanics and wet adhesion of pretarsal pads in ants. *Integrat. Compar. Biol.* 42, 1100–1106. doi: 10.1093/icb/42.6.1100

Fowler, J. E., Franz, J., Golbek, T. W., Weidner, T., Gorb, E. V., Gorb, S. N., and Baio, J. E. (2021). Surface chemistry of the ladybird beetle adhesive foot fluid across various substrates. *Biointerphases.* [Epub ahead of print].

Geiselhardt, S. F., Federle, W., Prüm, B., Geiselhardt, S., Lamm, S., and Peschke, K. (2010). Impact of chemical manipulation of tarsal liquids on attachment in the Colorado potato beetle, *Leptinotarsa decemlineata*. *J. Insect Physiol.* 56, 398–404. doi: 10.1016/j.jinsphys.2009.11.016

Geiselhardt, S. F., Geiselhardt, S., and Peschke, K. (2009). Comparison of tarsal and cuticular chemistry in the leaf beetle *Gastrophysa viridula* (Coleoptera: Chrysomelidae) and an evaluation of solid-phase microextraction and solvent extraction techniques. *Chemoecology* 19:185. doi: 10.1007/s00049-009-0021-y

Geiselhardt, S. F., Geiselhardt, S., and Peschke, K. (2011). Congruence of epicuticular hydrocarbons and tarsal secretions as a principle in beetles. *Chemoecology* 21:181. doi: 10.1007/s00049-011-0077-3

Gilet, T., Heepe, L., Lambert, P., Compere, P., and Gorb, S. N. (2018). Liquid secretion and setal compliance: the beetle's winning combination for a robust and reversible adhesion. *Curr. Opin. Insect Sci.* 30, 19–25. doi: 10.1016/j.cois.2018.08.002

Gorb, E., and Gorb, S. (2002). Attachment ability of the beetle *Chrysolina fastuosa* on various plant surfaces. *Entomol. Exp. Appl.* 105, 13–28. doi: 10.1046/j.1570-7458.2002.01028.x

Gorb, E., and Gorb, S. (2009). Effects of surface topography and chemistry of *Rumex obtusifolius* leaves on the attachment of the beetle *Gastrophysa viridula*. *Entomol. Exp. Appl.* 130, 222–228. doi: 10.1111/j.1570-7458.2008.00806.x

Gorb, E., Voigt, D., Eigenbrode, S. D., and Gorb, S. (2008). Attachment force of the beetle *Cryptolaemus montrouzieri* (Coleoptera, Coccinellidae) on leaflet surfaces of mutants of the pea *Pisum sativum* (Fabaceae) with regular and reduced wax coverage. *Arthropod Plant Interact.* 2, 247–259. doi: 10.1007/s11829-008-9049-0

Gorb, E. V., Hosoda, N., Miksch, C., and Gorb, S. N. (2010). Slippery pores: anti-adhesive effect of nanoporous substrates on the beetle attachment system. *J. R. Soc. Interface R. Soc.* 7, 1571–1579. doi: 10.1098/rsif.2010.0081

Gorb, S. N. (2001). *Attachment Devices of Insect Cuticle*. Dordrecht, The Netherlands: Kluwer Academic Publishers.

Gorb, S. N. (2011). "Biological fibrillar adhesives: functional principles and biomimetic applications," in *Handbook of Adhesion, Technology*, eds L. F. M. da Silva, A. Öchsner and R. D. Adams (Berlin, Heidelberg: Springer), 1410–1436.

Gorb, S. N., Schuppert, J., Walther, P., and Schwarz, H. (2012). Contact behaviour of setal tips in the hairy attachment system of the fly *Calliphora vicina* (Diptera, Calliphoridae): a cryo-SEM approach. *Zoology* 115, 142–150. doi: 10.1016/j.zool.2011.10.006

Gorb, S. N., Sinha, M., Peressadko, A., Daltorio, K. A., and Quinn, R. D. (2007). Insects did it first: a micropatterned adhesive tape for robotic applications. *Bioinspir. Biomim.* 2:S117. doi: 10.1088/1748-3182/2/4/S01

Gupta, S., Cochran, H., and Cummings, P. (1998). Nanorheology of liquid alkanes. *Fluid Phase Equilibr.* 150, 125–131. doi: 10.1016/S0378-3812(98)00283-0

Heepe, L., Wolff, J. O., and Gorb, S. N. (2016). Influence of ambient humidity on the attachment ability of ladybird beetles (*Coccinella septempunctata*). *Beilstein J. Nanotechnol.* 7, 1322–1329. doi: 10.3762/bjnano.7.123

Himmelhaus, M., Eisert, F., Buck, M., and Grunze, M. (2000). Self-assembly of n-alkanethiol monolayers. A study by IR-visible sum frequency spectroscopy (SFG). *J. Phys. Chem. B* 104, 576–584. doi: 10.1021/jp992073e

Hirose, C., Yamamoto, H., Akamatsu, N., and Domen, K. (1993). Orientation analysis by simulation of vibrational sum frequency generation spectrum: CH stretching bands of the methyl group. *J. Phys. Chem.* 97, 10064–10069. doi: 10.1021/j100141a028

Hosoda, N., and Gorb, S. N. (2012). Underwater locomotion in a terrestrial beetle: combination of surface de-wetting and capillary forces. *Proc. R. Soc. London B Biol. Sci.* 279, 4236–4242. doi: 10.1098/rspb.2012.1297

Korosi, G., and Kovats, E. S. (1981). Density and surface tension of 83 organic liquids. *J. Chem. Eng. Data* 26, 323–332. doi: 10.1021/je00025a032

Labonte, D., and Federle, W. (2015). Scaling and biomechanics of surface attachment in climbing animals. *Philos. Trans. R. Soc. B Biol. Sci.* 370:20140027. doi: 10.1098/rstb.2014.0027

Langer, M. G., Ruppersberg, J. P., and Gorb, S. (2004). Adhesion forces measured at the level of a terminal plate of the fly's seta. *Proc. R. Soc. London B Biol. Sci.* 271, 2209–2215. doi: 10.1098/rspb.2004.2850

Ludviksson, V., and Lightfoot, E. (1971). The dynamics of thin liquid films in the presence of surface-tension gradients. *AIChE J.* 17, 1166–1173. doi: 10.1002/aic.690170523

Ma, G., and Allen, H. C. (2006). DPPC Langmuir monolayer at the air-water interface: probing the tail and head groups by vibrational sum frequency generation spectroscopy. *Langmuir* 22, 5341–5349. doi: 10.1021/la0535227

Mo, H., Evmenenko, G., and Dutta, P. (2005). Ordering of liquid squalane near a solid surface. *Chem. Phys. Lett.* 415, 106–109. doi: 10.1016/j.cplett.2005.08.142

Moore, J., Cui, S., Cochran, H., and Cummings, P. (2000). Rheology of lubricant basestocks: a molecular dynamics study of C 30 isomers. *J. Chem. Phys.* 113, 8833–8840. doi: 10.1063/1.1318768

Niederegger, S., and Gorb, S. N. (2003). Tarsal movements in flies during leg attachment and detachment on a smoothe substrate. *J. Insect Physiol.* 49, 611–620. doi: 10.1016/S0022-1910(03)00048-9

Peisker, H., and Gorb, S. N. (2012). Evaporation dynamics of tarsal liquid footprints in flies (*Calliphora vicina*)and beetles (*Coccinella septempunctata*). *J. Exp. Biol.* 215 (Pt 8), 1266–1271. doi: 10.1242/jeb.065722

Peisker, H., Heepe, L., Kovalev, A. E., and Gorb, S. N. (2014). Comparative study of the fluid viscosity in tarsal hairy attachment systems of flies and beetles. *J. R. Soc. Interface* 11, 1–7. doi: 10.1098/rsif.2014.0752

Thornham, D. G., Blackwell, A., Evans, K. A., Wakefield, M., and Walters, K. F. A. (2008). Locomotory behaviour of the seven-spotted ladybird, *Coccinella septempunctata*, in response to five commonly used insecticides. *Ann. Appl. Biol.* 152, 349–359. doi: 10.1111/j.1744-7348.2008.00224.x

Tsige, M., and Patnaik, S. S. (2008). An all-atom simulation study of the ordering of liquid squalane near a solid surface. *Chem. Phys. Lett.* 457, 357–361. doi: 10.1016/j.cplett.2008.04.026

Vötsch, W., Nicholson, G., Müller, R., Stierhof, Y. D., Gorb, S., and Schwarz, U. (2002). Chemical composition of the attachment pad secretion of the locust *Locusta migratoria*. *Insect Biochem. Mol. Biol.* 32, 1605–1613. doi: 10.1016/S0965-1748(02)00098-X

Walker, G. (1993). Adhesion to smooth surfaces by insects—a review. *Int. J. Adhesion Adhesives* 13, 6–10. doi: 10.1016/0143-7496(93)90002-Q

Weidner, T., Apte, J. S., Gamble, L. J., and Castner, D. G. (2010). Probing the orientation and conformation of alpha-Helix and beta-strand model peptides on self-assembled monolayers using sum frequency generation and NEXAFS spectroscopy. *Langmuir* 26, 3433–3440. doi: 10.1021/la903267x

Weidner, T., and Castner, D. G. (2013). SFG analysis of surface bound proteins: a route towards structure determination. *Phys. Chem. Chem. Phys.* 15, 12516–12524. doi: 10.1039/c3cp50880c

Conflict of Interest: The authors declare that the research was conducted in the absence of any commercial or financial relationships that could be construed as a potential conflict of interest.